PHYSICAL REVIEW B **81**, 161201(R) (2010)

Point defect chemistry in amorphous HfO_2: Density functional theory calculations

C. Tang and R. Ramprasad*

Department of Chemical, Materials and Biomolecular Engineering, Institute of Materials Science, University of Connecticut, 97 North Eagleville Road, Storrs, Connecticut 06269, USA

(Received 18 January 2010; published 7 April 2010)

Neutral and charged native point defects in amorphous HfO_2 were studied using first-principles computations. Thermodynamically, positively charged O vacancies and negatively charged Hf vacancies are the most probable point defects over a large atomic and electronic chemical-potential range. Moreover, of all point defects, the positively charged O vacancy is the one with the lowest migration barrier. Hence, this point defect is identified as the most dangerous one in amorphous HfO_2 within the context of high-K gate dielectric applications in microelectronics.

DOI: 10.1103/PhysRevB.81.161201 PACS number(s): 66.30.Lw

The usage of metal-SiO_2-Si gate stacks has been pervasive in microelectronic devices for the last four decades with device miniaturization in successive generations achieved by simple physical scaling of the gate stack. Since continued device miniaturization through physical scaling has reached an impasse, the community is poised for the replacement of SiO_2 by HfO_2 based "high-K" dielectrics.[1,2]

Widespread usage of the new high-K gate stack is however expected to be hampered due to several troubling issues, including band bending in the Si substrate layer, and threshold voltage shifts. The causes of such undesirable effects have been attributed to the presence of unexplained charges or dipoles within the dielectric layer.[3] There is mounting evidence that intrinsic O defects in HfO_2 may be the culprits, as supported by experiments performed at varying levels of O exposure and anneals.[4] In particular, positively charged O vacancies appear to be the most significant and mobile native defects contributing to such unexpected and undesirable behavior.[5]

Concomitant with the above-mentioned technological evolution, the last decade has seen a number of detailed fundamental *ab initio* computational studies of monoclinic HfO_2 (m-HfO_2) involving dielectric phenomena,[6,7] phase equilibria,[8] and defect chemistry.[9–14] From a thermodynamic point of view, the most dominant point defects in m-HfO_2 are positively charged O and negatively charged Hf vacancies.[15] Kinetic considerations based on the point-defect migration barriers in m-HfO_2 however indicate that O interstitials[16] are more important than O vacancies[17] as the former have smaller barriers.

Recently, the more relevant (but also more challenging) amorphous HfO_2 (a-HfO_2) phase has been investigated using *ab initio* computational methods.[18–21] Treatment of the amorphous phase is appropriate not only because the as-deposited phase is amorphous but also due to the requirement that the HfO_2 layer be maintained in the amorphous phase.[2] Prior computational work indicate that the formation energies of O point defects are, in general, lower in a-HfO_2 than in m-HfO_2.[19–21]

In this paper, we present *ab initio* density functional theory (DFT) based calculations that address the formation *and* migration of O vacancy (O_v^q), O interstitial (O_i^q), and Hf vacancy (Hf_v^q) point defects in various charge states q in a-HfO_2. Since the behaviors of point defects are primarily determined by the local chemistry, which can be quite different in m-HfO_2 and a-HfO_2, the use of suitable structural models is critical to capture the characteristics of point defects. Our detailed analysis of point defects in various chemical and coordination environments permitted by the a-HfO_2 model lead us to the conclusion that positively charged O vacancies are indeed the most prevalent *and* mobile point defects—a conclusion that is expected to persist even when more accurate beyond-DFT computations are utilized.

Our DFT calculations were performed using the VASP code[22] with Vanderbilt ultrasoft pseudopotentials,[23] the PW91 generalized gradient approximation[24] and a cutoff energy of 400 eV for the plane-wave expansion of the wave functions. A Monkhorst-Pack k-point sampling mesh of $2\times2\times2$ was used in all of our calculations, which involved 32 HfO_2 units per supercell. Figure 1 (top) shows the a-HfO_2 model used here, created elsewhere using the melt-and-quench method.[18] Comparison between the coordination number distributions in a-HfO_2 and m-HfO_2 [Fig. 1 (bottom)] indicates that the local environments of both O and Hf are quite different in these two phases.

O vacancies and interstitials at eight threefold and eight fourfold sites, and Hf vacancies at four sixfold and five sevenfold sites were considered to provide a statistically meaningful understanding of defect chemistry. Migration pathways involving all these sites were also considered and barriers for migration were determined using the elastic-band method.[25] For definiteness, only the pathways that connect one end of the supercell to the opposite end [see Fig. 1 (top)] are discussed. One may expect the unambiguous identification (or definition) of a point defect in an amorphous environment to be tricky. In the case of a-HfO_2, the neutral O vacancy in a-HfO_2 maintains its localized defect state in the band gap of HfO_2 even after molecular dynamics at 2000 K.[21] However, the unoccupied defect state displayed in the band gap by the 2+ charged O vacancy after 0 K minimization is "lost" to the HfO_2 conduction band after molecular dynamics at 2000 K.[21] Nevertheless, a-HfO_2 appears to allow a reversible (structural and energetic) transformation between the charged to the uncharged state;[21] thus, in this restricted sense, one may view the point defects as having their respective identities.

We begin by commenting about the relative stability of

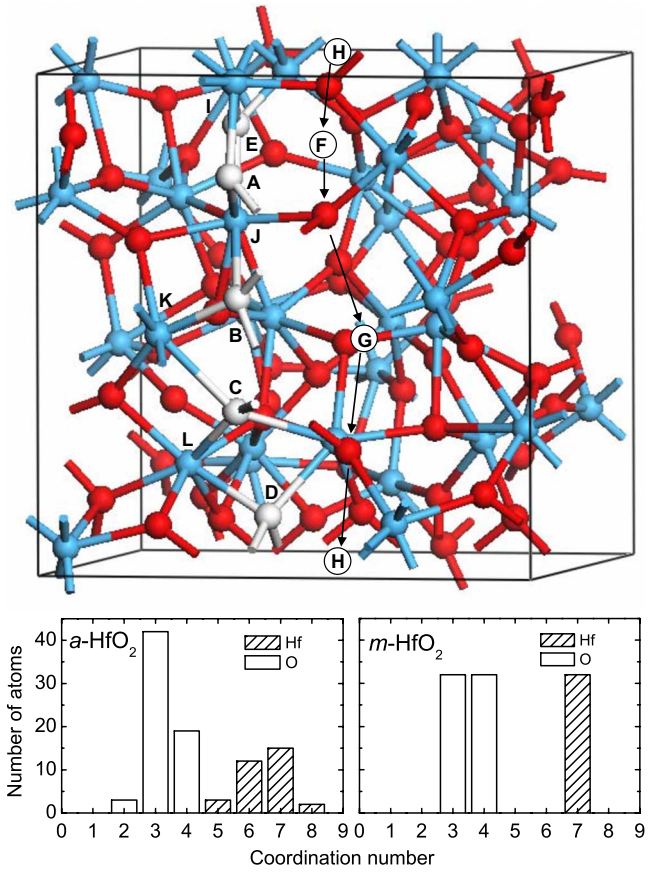

FIG. 1. (Color online) Top: model of a-HfO_2. Hf: blue (gray), O: red (dark gray) or white. The long-range migration path for O vacancies is represented by the O sites A-E (highlighted in white), the path for O interstitials schematically by circles F-H, and the path for Hf vacancies by Hf sites I-L. Bottom: coordination number distribution in a-HfO_2 and m-HfO_2 containing 32 HfO_2 units per supercell.

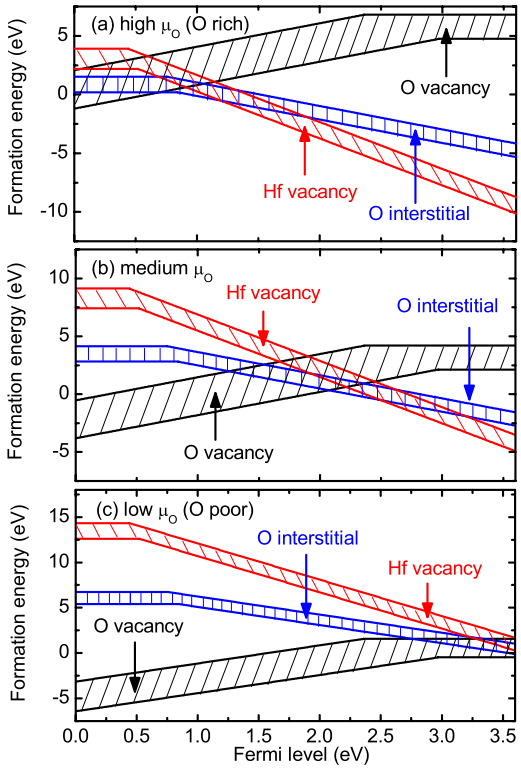

FIG. 2. (Color online) Formation energies for various types of point defects in a-HfO_2 as a function of electronic chemical potential (i.e., the Fermi level) and for three choices of O chemical potential, (a) spanning high, (b) medium, and (c) low values. Shaded bands are intended to capture the range of formation-energy values possible in a-HfO_2. The horizontal bands are for neutral defects (O_v^0, O_i^0, and Hf_v^0) and the sloped ones are for charged defects (O_v^{2+}, O_i^{2-}, and Hf_v^{4-}). The Fermi level is referenced to the valence-band maximum.

O_v^q, O_i^q, and Hf_v^q defects in neutral states ($q=0$). The formation energies, E_f, of O_v^0 in the threefold and fourfold sites were determined to be 4.7–6.8 eV and 5.3–6.8 eV, respectively, compared to the corresponding values of 6.42 and 6.40 eV for the m-HfO_2 phase.[9] An O_i^0 defect tends to form a covalent dimer with a lattice O in its attempt to achieve saturation; in a-HfO_2, the bond length of O-O dimer was determined to be in the 1.5–1.6 Å range, compared to 1.5 Å in m-HfO_2. E_f for O_i^0 bound to threefold lattice O sites were determined to be in the 0.7–1.5 eV range, lower than the corresponding value of 1.6 eV in m-HfO_2. This is not surprising as there is more open volume to accommodate interstitials in a-HfO_2. E_f for O_i^0 near the fourfold sites were much higher (1.2–2.4 eV), consistent with the smaller space in the neighborhood of these sites. The extra space around twofold O sites decreases E_f to 0.20–0.45 eV. However, due to the very low fraction of twofold O sites in a-HfO_2, and the high E_f values for fourfold sites, we extensively consider only threefold sites in this study. We note that our computed formation energies for neutral O defects in a-HfO_2 are in good agreement with prior predictions.[19,21] E_f of Hf_v^0 was calculated to be 2.2–3.9 eV, much lower than the counterpart value (5.9 eV) in m-HfO_2.[9] In the above discussion on neutral point defects, the chemical potential of O (μ_O) was taken to be half the DFT energy of an O_2 molecule, and that of Hf (μ_{Hf}) was defined as $E_{HfO_2}-2\mu_O$, where E_{HfO_2} is the energy per HfO_2 unit in a-HfO_2.

The above choices of chemical potentials (or "reference energies") were made to allow for a direct comparison of the E_f values in a-HfO_2 computed here to prior m-HfO_2 results. In fact, these μ_O and μ_{Hf} choices correspond to "O rich" or "high μ_O" conditions.[15] The other extreme, namely, "O poor" or "low μ_O" conditions occurs when μ_{Hf} is taken to be the energy per Hf atom of bulk hcp Hf, and $\mu_O=0.5\times(E_{HfO_2}-\mu_{Hf})$.[15] Depending on the ambient conditions, μ_O may vary between these extreme values, and consequently, the relative stability of the different types of defects may also vary. Also, depending on the energetic placement and occupancies of point-defect states in the band gap, charged defects are expected to be stable at appropriate electronic chemical-potential (i.e., the Fermi-level) values. Following procedures used for treating different charge states and different types of point defects,[26] the dependence of E_f for the three types of defects under study as a function of the O and electronic chemical potentials were determined, as shown in Fig. 2. The multipole interactions between the charged de-

fects and their image charges were treated using the first-order Makov-Payne correction.[27] Although several different charge states for each type of point defect were considered, only results corresponding to the neutral defects and those corresponding to the most stable charge state for each type of point defect, namely, O_v^{2+}, O_i^{2-}, and Hf_v^{4-}, are shown for clarity. It can be seen that the O_v^{2+} and Hf_v^{4-} are the most stable across a wide range of electronic and O chemical potentials.

It is worth pointing out that charging of point defects result in expected changes in the physical structure. For instance, the loss of electrons during the charging of O_v^0 results in the outward movement of the neighboring Hf ions away from the vacancy by 0.2 Å on average and the substantial inward relaxation of the surrounding O ions. On the other hand, successive electron trapping by O_i^0 decreases the tendency for pairing of the interstitial with a lattice O, resulting in increased O-O dimer bond lengths of 2.2–2.4 and 2.3–2.5 Å for the 1- and 2-charge states, respectively. Similarly, one would expect that Hf_v^{4-} substantially repels its neighboring O ions and attracts other Hf ions due to its high charge state. However, this occurs only for a few Hf_v^{4-} in our sampling and on average we found no significant structural differences from the neutral case. For example, it was found that only about 8% of the Hf cations move by more than 0.2 Å toward the Hf vacancy when it gets charged. This abnormal behavior might result from the large neighboring Hf-Hf distances, which weaken the Coulomb interaction. As we shall see below, the change in the local structure of point defects due to charging has significant implications for their migration behavior.

With the formation of point defects (thermodynamics) addressed, now we discuss the migration of these defects (kinetics) in *a*-HfO_2. As noted earlier, although several different elementary steps connecting nearest-neighbor point-defect sites were studied, only migration pathways that connect one end of the supercell to the opposite end are presented here. In constructing such "long-range" diffusion pathways, an attempt was made to include elementary steps with the smallest barriers. First, we discuss O vacancy diffusion using the diffusion loop path $A \rightarrow B \rightarrow C \rightarrow D \rightarrow E \rightarrow A$ [Fig. 1 (top)]. The energy profiles of both O_v^0 and O_v^{2+} diffusion along this path are shown in Fig. 3 (top). The minima of the profiles represent local stable equilibria and the maxima being saddle points, or migration barriers, for each elementary step. All energies are defined with respect to the absolute minimum for each charge state. It can be seen that the migration barrier drops drastically (by 1.0–1.5 eV) as a result of charging with the overall barrier for the entire pathway (defined as the energy difference between the absolute maximum and minimum of the profiles shown) dropping from 2.8 to 1.9 eV.

The large-barrier difference between O_v^0 and O_v^{2+} can be rationalized in terms of the local structure around the defects. In the O_v^{2+} case, the distance traveled by the hopping O between two neighboring vacancy sites is much shorter than that in the O_v^0 case as O_v^{2+} substantially attracts the surrounding O ions toward itself, as pointed out above. Moreover, the outward movement of the Hf cation away from the O vacancy due to positive charging results in an increase in the distance between the two Hf cations linking adjacent O vacancy sites (thereby providing more room for the migrating vacancy). The decrease in distance between adjacent O vacancy sites and the increase in the Hf-Hf distance due to charging are listed in Fig. 3 (top) for each of the elementary steps.

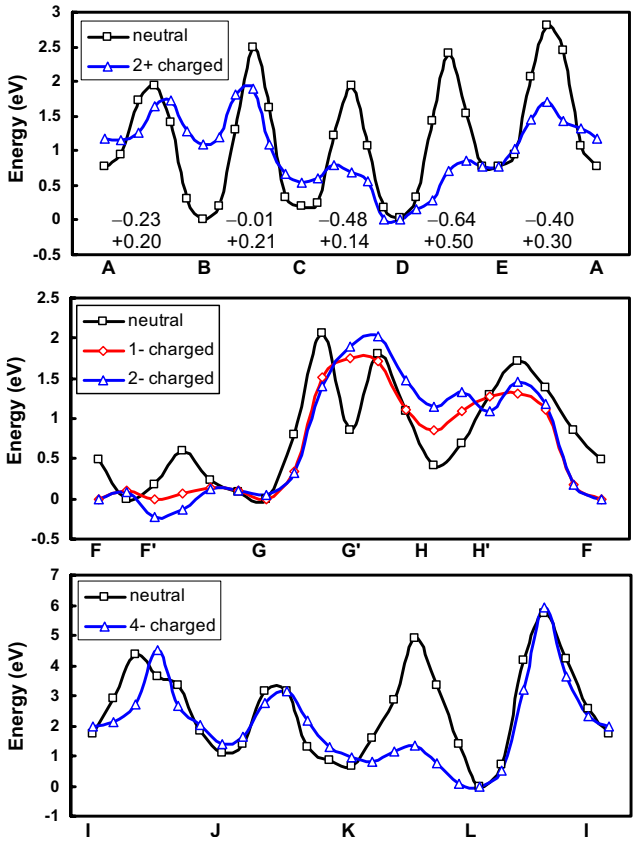

FIG. 3. (Color online) Energy profiles for point-defect migration in *a*-HfO_2. Top: O vacancy. Middle: O interstitial. Bottom: Hf vacancy. For the O vacancy case, the decrease in distance (Å) between adjacent O vacancy sites (negative values) and the increase in the Hf-Hf distance (positive values) due to charging are listed for each of the elementary steps.

In *a*-HfO_2 the lattice O ions surrounding an O interstitial form a "cage" and the interstitial can easily move around within the cage because of the short hopping distance, especially in the charged case. However, this movement does not contribute to the long-range diffusion of the interstitial. In order to study the contributing hopping steps, we consider a migration path $F \rightarrow G \rightarrow H \rightarrow F$, as shown in Fig. 1 (top). We note that O interstitial migration can occur either via the exchange mechanism, i.e., when the interstitial replaces a lattice O with the latter becoming the new interstitial, or via the interstitial mechanism, i.e., direct hopping of the interstitial.[16] Although both mechanisms were considered, we note that barriers were smallest when steps $F \rightarrow G$ and $G \rightarrow H$ occur via the exchange mechanism, and step $H \rightarrow F$ occurs via the interstitial mechanism. The energy profiles of O_i^0, O_i^-, and O_i^{2-} diffusion along the prescribed path are plotted in Fig. 3 (middle), in a similar manner to the O vacancy case. Although less stable than O_i^{2-}, O_i^- was considered as it exhibits a lower migration barrier in *m*-HfO_2.[16]

For the O_i^0 case, we can see that the hopping steps

F→G and G→H, via the exchange mechanism, have barriers of 0.6 and 2.1 eV, respectively. In these two steps, two intermediate configurations F′ and G′ with local minimum energies were found. These intermediate local minima result from the O-O dimer formed by the two hopping O. It is interesting to note that the local structure in a-HfO_2 allows the formation of O-O dimer during migration via the exchange mechanism, which is not the case in m-HfO_2.[16] Step H→F, via the interstitial mechanism, has an intermediate barrier 1.1 eV. The overall barrier for O_i^0 diffusion along the loop path is 2.1 eV. For the charged interstitial O_i^- and O_i^{2-}, the reduced tendency to form the O-O dimer results in the disappearance of the local minimum configuration G′. However, the local minimum F′ still persists. This also occurs in the O_i^{2-} migration step H→F, in which the hopping O bonds with its neighboring Hf cations and results in a local minimum H′. For both O_i^- and O_i^{2-}, the overall barriers are around 2.2 eV, close to the neutral one.

For Hf vacancy diffusion we considered the path I→J→K→L→I, which consists of the dominant sevenfold Hf sites, as shown in Fig. 1 (top). For Hf_v^0 migration along this path, the lowest and highest barriers for elementary steps are 2.1 and 5.7 eV, respectively, and the overall barrier is 5.7 eV, as shown in Fig. 3 (bottom). For Hf_v^{4-}, the overall barrier is also 5.7 eV, and for most elementary steps, the barrier heights resemble those of Hf_v^0. This is not surprising since the change in the local structure of Hf vacancy upon charging is generally small. For example, for step J→K, the travel distance of the hopping Hf is decreased by 0.14 Å (from 2.49 to 2.35 Å) upon charging. However, for step K→L, where the travel distance decreased by 0.92 Å (from 3.25 to 2.33 Å) upon charging, we did find a huge barrier decrease of more than 3 eV. However, as pointed out earlier, structural relaxations around an Hf vacancy due to charging are rare. Hence, such large-barrier reductions are not expected in general.

The diffusion paths presented in Fig. 3 are only a subset of all the paths studied. However, they are representative of the multitude of possibilities and enlightening. To summarize, the migration barriers of O vacancies drop drastically to rather small values during positive charging while those of the O interstitials and Hf vacancies change little during negative charging. Overall, the migration barriers of the positively charged O vacancies (O_v^{2+}) are the smallest and those for the Hf vacancies are the highest in a-HfO_2. These results, when combined with our thermodynamic analysis of the defect formation energies, lead to the conclusion that the O_v^{2+} defects are the most predominant *and* the most mobile in a-HfO_2.

Financial support through a grant from the National Science Foundation (NSF) and computational support through a NSF Teragrid Resource Allocation are gratefully acknowledged. The authors also thank David Vanderbilt for sharing the atomic coordinates of a-HfO_2 (Ref. 18).

*rampi@ims.uconn.edu

[1] M. Houssa, L. Pantisano, L.-Å. Ragnarsson, R. Degraeve, T. Schram, G. Pourtois, S. De Gendt, G. Groeseneken, and M. M. Heyns, Mater. Sci. Eng. R. **51**, 37 (2006).
[2] J. Robertson, Rep. Prog. Phys. **69**, 327 (2006).
[3] J. K. Schaeffer, L. R. C. Fonseca, S. B. Samavedam, Y. Liang, P. J. Tobin, and B. E. White, Appl. Phys. Lett. **85**, 1826 (2004).
[4] D. Lim, R. Haight, M. Copel, and E. Cartier, Appl. Phys. Lett. **87**, 072902 (2005).
[5] S. Guha and V. Narayanan, Phys. Rev. Lett. **98**, 196101 (2007).
[6] X. Zhao and D. Vanderbilt, Phys. Rev. B **65**, 233106 (2002).
[7] N. Shi and R. Ramprasad, Appl. Phys. Lett. **91**, 242906 (2007).
[8] V. Fiorentini and G. Gulleri, Phys. Rev. Lett. **89**, 266101 (2002).
[9] A. S. Foster, F. Lopez Gejo, A. L. Shluger, and R. M. Nieminen, Phys. Rev. B **65**, 174117 (2002).
[10] K. Xiong and J. Robertson, Microelectron. Eng. **80**, 408 (2005).
[11] J. Robertson, O. Sharia, and A. A. Demkov, Appl. Phys. Lett. **91**, 132912 (2007).
[12] J. L. Gavartin, D. M. Ramo, A. L. Shluger, G. Bersuker, and B. H. Lee, Appl. Phys. Lett. **89**, 082908 (2006).
[13] C. Tang and R. Ramprasad, Appl. Phys. Lett. **91**, 022904 (2007); **92**, 182908 (2008); Phys. Rev. B **75**, 241302(R) (2007).
[14] C. Tang, B. Tuttle, and R. Ramprasad, Phys. Rev. B **76**, 073306 (2007).
[15] J. X. Zheng, G. Ceder, T. Maxisch, W. K. Chim, and W. K. Choi, Phys. Rev. B **75**, 104112 (2007).
[16] A. S. Foster, A. L. Shluger, and R. M. Nieminen, Phys. Rev. Lett. **89**, 225901 (2002).
[17] N. Capron, P. Broqvist, and A. Pasquarello, Appl. Phys. Lett. **91**, 192905 (2007).
[18] D. Ceresoli and D. Vanderbilt, Phys. Rev. B **74**, 125108 (2006).
[19] C. Kaneta and T. Yamasaki, Microelectron. Eng. **84**, 2370 (2007).
[20] P. Broqvist and A. Pasquarello, Microelectron. Eng. **84**, 2022 (2007).
[21] P. Broqvist, A. Alkauskas, and A. Pasquarello, Appl. Phys. Lett. **92**, 132911 (2008).
[22] G. Kresse and J. Furthmuller, Phys. Rev. B **54**, 11169 (1996).
[23] D. Vanderbilt, Phys. Rev. B **41**, 7892 (1990).
[24] J. P. Perdew, J. A. Chevary, S. H. Vosko, K. A. Jackson, M. R. Pederson, D. J. Singh, and C. Fiolhais, Phys. Rev. B **46**, 6671 (1992).
[25] G. Henkelman and H. Jonsson, J. Chem. Phys. **113**, 9978 (2000).
[26] C. G. Van de Walle and J. Neugebauer, J. Appl. Phys. **95**, 3851 (2004).
[27] G. Makov and M. C. Payne, Phys. Rev. B **51**, 4014 (1995).